

Reduction of thermal conductance in two-dimensional phononic crystals by coherent phonon scattering

Roman Anufriev¹ and Masahiro Nomura^{1,2,*}

¹*Institute of Industrial Science, University of Tokyo, Tokyo, 153-8505, Japan*

²*Institute for Nano Quantum Information Electronics, University of Tokyo, Tokyo, 153-8505, Japan*

*Email address: nomura@iis.u-tokyo.ac.jp

The impact of lattice type, period, and filling fraction of two-dimensional silicon phononic crystals on thermal conductance at low temperatures is investigated systematically using the theory of elasticity and finite element method. Changes in the period and filling fraction of the phononic crystal significantly affect the group velocity and density of states of the phonons and, as a consequence, reduce the thermal conductance of the structure. The reduction does not depend significantly on the lattice type of phononic crystals, despite the differences in symmetry and geometry. The possibilities of experimental observation of this effect are discussed, and a mode of separating coherent from incoherent scattering is proposed. Moreover, the temperature dependence of coherent scattering is assessed, and our results demonstrate that coherent scattering plays an important role in realistic nanostructures only at relatively low temperatures.

I. INTRODUCTION

Phononic nanostructures are regarded as possible candidates for applications involving phonon management [1–3], due to the possibility to manipulate the flux of vibrational energy (i.e., heat or sound) by band engineering. Indeed, on the one hand, phononic crystals may exhibit complete phononic bandgaps, i.e., regions of frequency where the propagation of elastic waves is forbidden in any direction; the physics of this phenomenon has been investigated both theoretically [3–9] and experimentally [5,10] in various types of two-dimensional (2D) phononic crystals. On the other hand, Bragg diffraction and local resonances in the periodic media result in the flattening of branches in phonon dispersion in a wide range of frequencies. This change of phonon dispersion leads to changes of the group velocities of phonons [11–13] and the density of states (DOS) [11,13–15]. These effects originate from the wave nature of phonons and are associated with coherent scattering, which is the process when phonons preserve their phase after a scattering event, in contrast to various incoherent scattering processes when phonons do not preserve their phase. Such modifications of phonon dispersion are thought to have the ability to reduce the thermal conductivity of nanostructures, in addition to reduction by incoherent scattering mechanisms such as surface [16–18], impurity [19], and Umklapp [17,20] scattering processes. Recent experiments demonstrated very low values of thermal conductivity at room

temperature in freestanding thin-film silicon nanostructures with 2D square [14,21] and hexagonal [22] arrays of holes. To explain these low values of thermal conductivity, Dechaumphai *et al.* [12] developed a model that takes into account both coherent and incoherent scattering mechanisms, and Lacatena *et al.* [23] used a molecular dynamic approach, whereas Jain *et al.* [24] argued that coherent scattering is unlikely to appear at room temperature and some of these experimental results could be explained by treating phonons as particles with bulk properties. However, Zen *et al.* [11] demonstrated that, in 2D phononic structures, at sub-kelvin temperatures, thermal conductance is totally controlled by coherent modifications of phonon dispersion, while incoherent mechanisms play a negligible role. An overview of recent theoretical and experimental investigations shows that coherent scattering of phonons can play an important role in heat transport, while its dependence on the geometry and temperature of the structure remains a disputable matter. No systematic theoretical studies of this effect are available in the literature.

In this study, we use the theory of elasticity and finite element method (FEM) to investigate theoretically the impact of the phononic structure design on the reduction of the group velocity and DOS. We demonstrate the dependence of thermal conductance on the period, radius-to-period ratio, and lattice type of the phononic structure. Moreover, we study the temperature dependence of this effect and discuss its occurrence in realistic nanostructures at different temperatures.

II. SIMULATION OF PHONONIC CRYSTALS

We simulate infinite periodic arrays of holes in thin freestanding silicon membranes [Fig. 1(a)] with various periods (a) and hole radii (r). An infinite structure is simulated by considering a three-dimensional unit cell of finite thickness (h) with Floquet periodic boundary conditions applied on the x - y plane [6]. At the low temperature limit, the wavelengths of phonons are longer than the characteristic scale of the system. Thus, we can use classical elasticity theory to compute the phonon modes. We use FEM, implemented by COMSOL MULTIPHYSICS® v4.4 software, to calculate numerically the eigenfrequencies from the elastodynamic wave equation:

$$\mu \nabla^2 \mathbf{u} + (\mu + \lambda) \nabla (\nabla \cdot \mathbf{u}) = -\rho \omega^2 \mathbf{u}, \quad (1)$$

with \mathbf{u} as the displacement vector, $\rho = 2329 \text{ kg m}^{-3}$ as the mass density, and $\lambda = 84.5 \text{ GPa}$ and $\mu = 66.4 \text{ GPa}$ as the Lamé parameters of silicon. First we calculate the eigenfrequencies for the wave vectors at the periphery of the irreducible triangle of the first Brillouin zone (BZ) [Fig. 1(b)], and then we evaluate the eigenfrequencies in the interior of the BZ as

an extrapolation of the values at the periphery within the triangle [Fig. 1.(c)] [25]. To study the heat transport through the structure, we calculate the heat flux spectra $Q(\omega, T)$ at a given temperature (T) as:

$$Q(\omega, T) \propto \frac{\hbar\omega D(\omega)v_{gr}(\omega)}{\exp(\hbar\omega/k_bT)-1}, \quad (2)$$

where $v_{gr}(\omega)$ is the average group velocity, $D(\omega)$ is the total DOS calculated over the entire BZ, with close attention to the band intersections, and k_b is the Boltzmann constant [26]. More details on our theoretical approach can be found in Ref. [13]. Figures 1(d), 1(e), and 1(f) show typical spectra of the group velocity, DOS, and heat flux calculated from the obtained band diagram.

For the purpose of comparison, we also present the data for an unpatterned membrane of the same thickness. The dispersion of the membrane can also be obtained from analytic Rayleigh–Lamb equations [27]. Comparing the heat flux calculated from analytically obtained dispersion and the dispersion obtained numerically by COMSOL MULTIPHYSICS®, we estimate the maximum inaccuracy of this calculation to be about 5–15%, depending on the lattice type. In order to remove the part of the error originating from the difference in lattice type, we divide the thermal conductance of each lattice by that of the membrane calculated using the BZ of the same lattice type. Moreover, we simulate the same structures as those studied in the literature [4,6,11,12,28] to verify the validity of our calculation and find our results in agreement with the obtained band diagrams, group velocity, and DOS spectra.

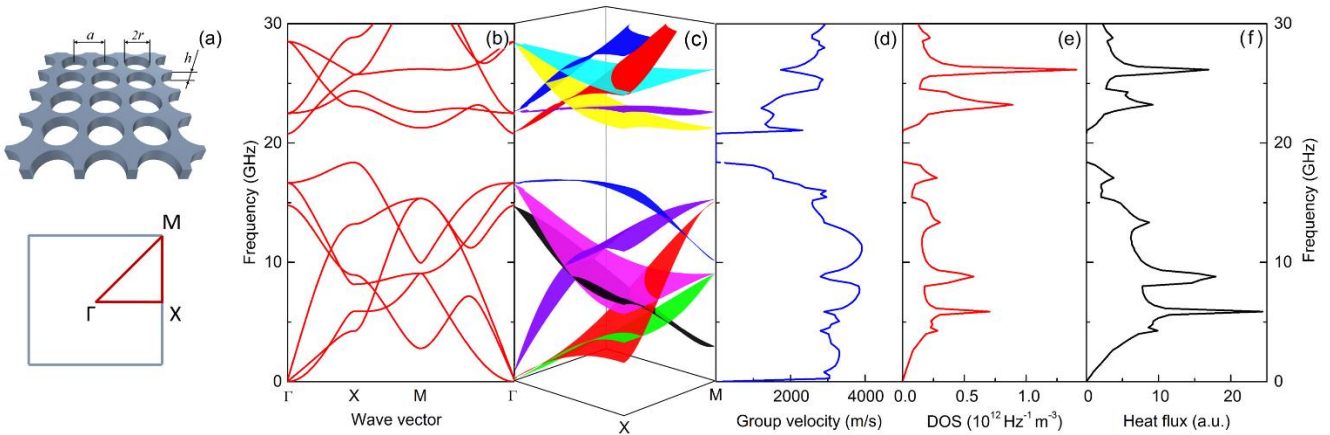


FIG. 1. (Color online) (a) Scheme of the simulated structure, its unit cell, and the first BZ with the high symmetry points: Γ (0, 0), X (π/a , 0), and M (π/a , π/a). (b) Unsorted band diagram of the structure with $a = 160$ nm, $r/a = 0.45$, and $h = 80$

nm plotted at the high symmetry points. (c) Sorted band diagram plotted in the interior of the irreducible triangle of the first BZ. Spectra are shown for (d) the average group velocity, (e) DOS, and (f) heat flux.

III. IMPACT OF THE DESIGN

We study three different types of lattice: square, hexagonal [Fig. 2(a)], and honeycomb [Fig. 2(b)]. Figures 2(c) and 2(d) show the corresponding phonon dispersions of hexagonal and honeycomb lattices, respectively. Despite the similarities between the lattices, the band diagrams are completely different. However, the corresponding spectra of the heat flux are very similar, as shown in Figs. 2(e) and 2(f). Analyzing the appearance of the phononic bandgap in the different lattices, we find the same trends as those known from the literature [4,8,9,11,28,29]: the width of the bandgap increases as a function of the r/a ratio, and the widest bandgap is expected for the honeycomb lattice, while, as a function of the h/a ratio, the widest bandgaps are expected at around the values of 0.5 and 1. However, the bandgap alone may play only a minor role in the suppression of thermal conductance at temperatures above the sub-kelvin range, as is evident from the heat flux spectrum at 1 K [Fig. 2(f)]: the region covered by the bandgap is very small, as compared to the whole range of frequencies. For this reason, we focus our study on the changes in the group velocity and DOS.

To illustrate this effect, we consider two square lattice nanostructures with the same thickness ($h = 80$ nm) and r/a ratios (0.4), but different periods ($a = 80$ and 320 nm). Figure 3(a) demonstrates that both phononic structures show significant reduction of the group velocity, as compared to the membrane, but this reduction is larger in the structure with a longer period ($a = 320$ nm). This phenomenon is a direct consequence of band flattening in phononic crystals [11,12,30]. The DOS of the phononic structures are similar to that of the membrane. Yet again, the structure with a longer period demonstrates a lower DOS [Fig. 3(b)]. As a consequence, the heat flux, which is proportional to the product of the group velocity and DOS, shows a reduction for both phononic structures, as compared to the membrane, except for the low frequency part [13] [Fig. 3(c)]. This reduction is stronger in the structure with a longer period, due to the lower DOS spectrum. The same effect is observed also in hexagonal and honeycomb lattices. This result is consistent with recent experimental and theoretical data where the heat flux in SiN phononic structures was also reduced significantly as the period was increased [11].

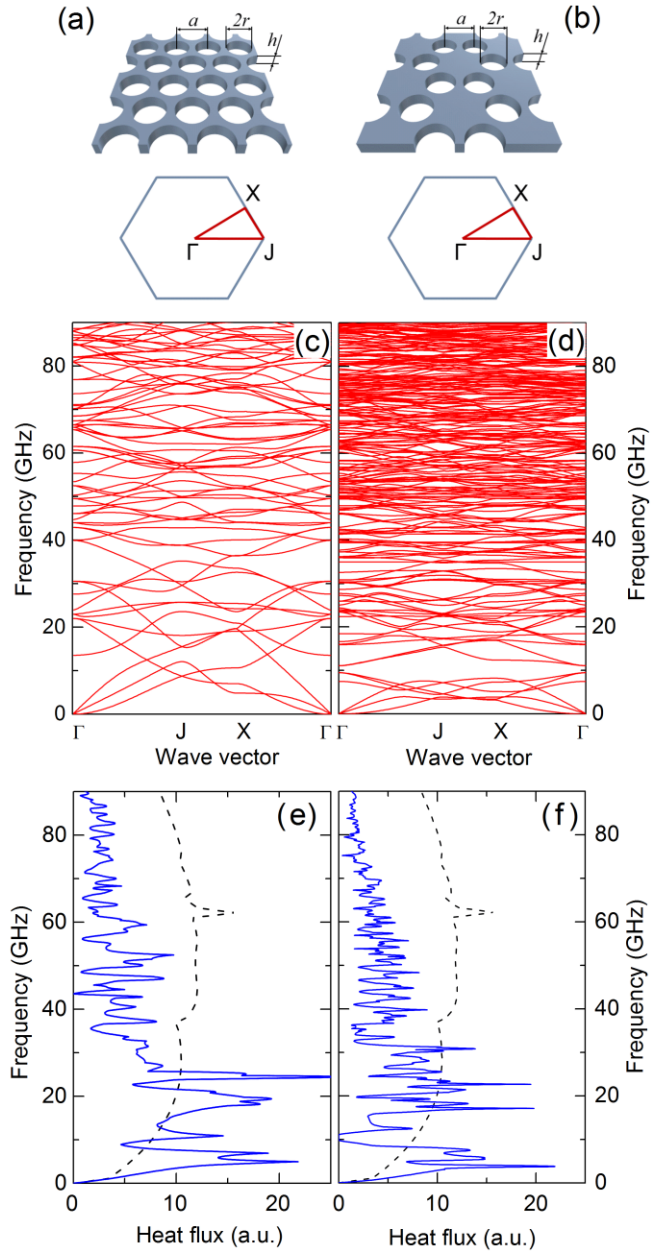


FIG. 2. (Color online) Schemes of the structures and first BZs with high symmetry points for (a) hexagonal lattice: Γ (0, 0), J ($4\pi/3a, 0$), and X ($\pi/a, \pi/\sqrt{3}a$), and (b) honeycomb lattices: Γ (0, 0), J ($4\pi/3\sqrt{3}a, 0$), and X ($\pi/\sqrt{3}a, \pi/\sqrt{3}a$). The band diagrams are shown for (c) hexagonal and (d) honeycomb structures ($r/a = 0.45$, $a = 160$ nm, and $h = 80$ nm), and (e, f) the corresponding spectra of heat flux, calculated at 1 K for the phononic crystals (solid line) and an unpatterned membrane (dashed line).

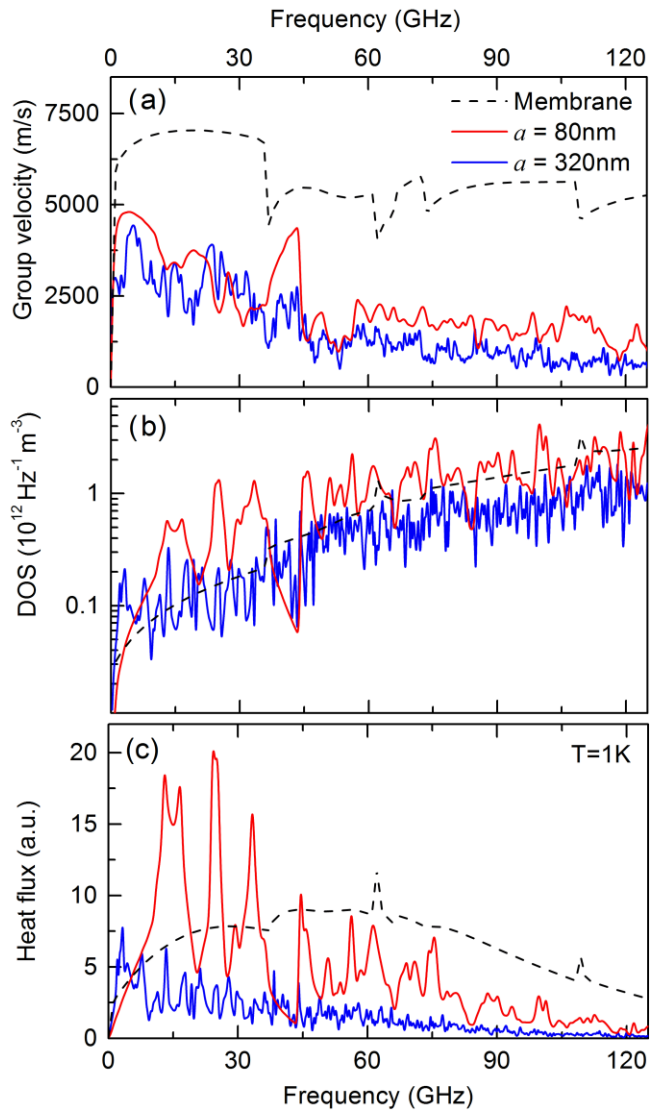


FIG. 3. (Color online) Spectra of (a) the average group velocity, (b) the DOS, and (c) the heat flux at 1 K, calculated for the membrane (dashed line) and square lattice structures with periods $a = 80$ nm (red solid line) and $a = 320$ nm (blue solid line), and $r/a = 0.40$ for both structures. The thickness of the membrane and phononic structures is 80 nm.

To compare quantitatively structures with different designs, we evaluate the integral of the heat flux spectra up to the highest available states at 1 K: $G(T) = \int Q(\omega, T) d\omega$. This quantity is proportional to the thermal conductance of the structure. Figure 4 shows the reduction of thermal conductance in phononic structures of different designs, as compared to that of an unpatterned membrane: $(G_{Mem} - G_{PnC}) / G_{Mem}$, where G_{PnC} and G_{Mem} are the thermal conductance of phononic crystals and a membrane, respectively. As a function of the period (with constant r/a), the reduction of thermal conductance is increased for the structures of all lattice types [Fig. 4(a)]. In contrast, in the phononic structures with a relatively small period ($a < 60$ nm), the thermal conductance is enhanced. This thermal conductance boost effect is studied in detail in Ref. [13]. These data imply that, in the presence of coherent scattering, a reduction of the period does not

result necessarily in a more efficient phonon scattering, as expected from incoherent surface scattering due to an increase of the surface-to-volume ratio [16,21].

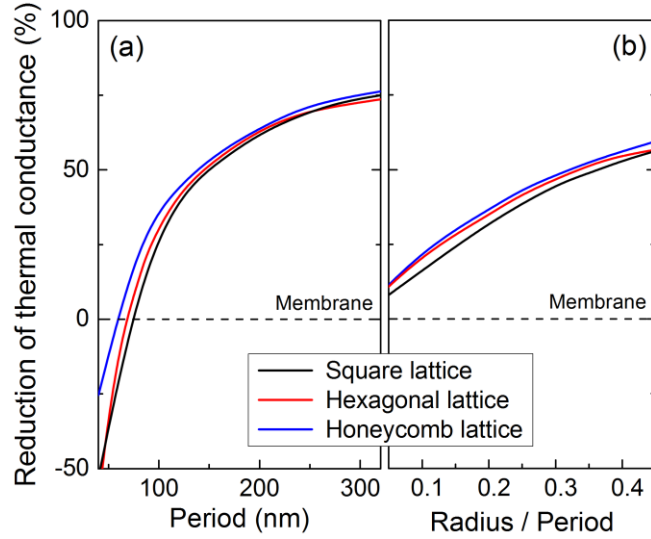


FIG. 4. (Color online) Reduction of thermal conductance $(G_{Mem} - G_{PnC}) / G_{Mem}$ in phononic structures with square, hexagonal, and honeycomb lattices, as compared to an unpatterned membrane of the same thickness ($h = 80$ nm), calculated at 1 K as (a) a function of period a with constant $r/a = 0.4$ and (b) a function of the r/a ratio with constant $a = 160$ nm. To obtain each curve 8 (a) and 7 (b) different structures were calculated.

Figure 4(b) shows the reduction of thermal conductance as a function of the r/a ratio at a constant period of 160 nm. All three lattices demonstrate the same increasing trend with an increase of the hole radius. Therefore, the strongest reduction of thermal conductance takes place in the structures with the highest r/a ratio possible, since it is optimal for both coherent and incoherent [16,18,24] scattering mechanisms. It is important to note that the structures with the same radius and period, but different lattice type, have nearly the same values of thermal conductance [Fig. 4]. This fact might be related to the presence of local resonances which may be similar in different lattices and partly can form the dispersion of the structures [6]. However, this finding implies that the choice of the lattice type can be made in order to achieve the best mechanical or electrical properties or the strongest incoherent surface scattering.

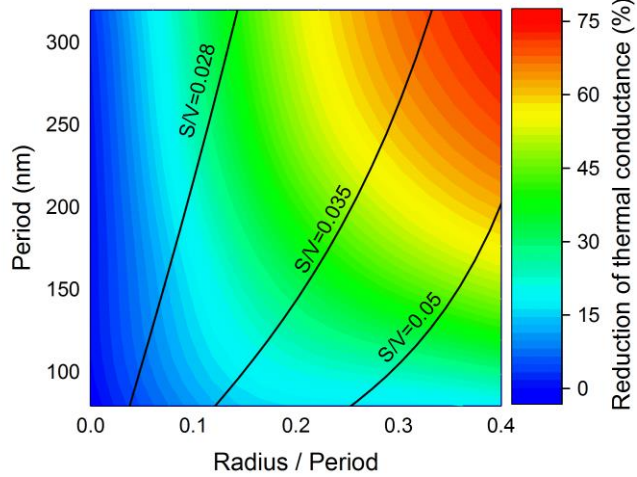


FIG. 5. (Color online) Reduction of thermal conductance $(G_{Mem} - G_{PnC}) / G_{Mem}$ in square lattice phononic crystals as a function of the period and radius-to-period ratio at a temperature of 1 K. Black solid curves show the lines of constant surface-to-volume ratio (S/V).

As far as incoherent phonon scattering mechanisms are concerned, one of the dominant mechanisms in pure monocrystalline nanostructures is surface scattering, especially at low temperatures [17,31]. As a consequence, the thermal conductance in nanostructures is proportional to the surface-to-volume ratio. To study the dependence of coherent scattering on the surface-to-volume ratio, we extended our calculation to structures with various values of a and r/a , and obtained the intermediate points by interpolation. Figure 5 shows the map of thermal conductance reduction by coherent scattering in various square lattice structures at 1 K, together with the lines of constant surface-to-volume ratio. From a coherent scattering perspective, the reduction of thermal conductance is increased with increasing a and/or r/a , while, from an incoherent scattering perspective, the surface scattering should be constant along each line of constant surface-to-volume ratio and become stronger as the surface-to-volume ratio is increased. Therefore, the best way to study the impact of coherent scattering on thermal conductance experimentally would be to compare the structures of the same surface-to-volume ratio, so that the impact of the incoherent surface scattering is isolated from the coherent one.

IV. TEMPERATURE DEPENDENCE

Since heat flux depends on the Bose–Einstein distribution, this implies that temperature must affect thermal conductance significantly. Figure 6(a) shows the temperature dependence of the reduction in thermal conductance of phononic crystals with different periods, as compared to an unpatterned membrane. At the low temperature limit, the thermal conductance of phononic crystals approaches, and even overcomes, that of the membrane, which again reflects

the thermal conductance boost effect [13]. As the temperature is increased, the reduction also is increased towards the 100% limit for all periods. This is explained by the fact that, at higher temperatures, the Bose–Einstein distribution allows the occupation of higher-frequency states where the values of the group velocities and DOS in phononic crystals are lower than those in an unpatterned membrane (Fig. 3).

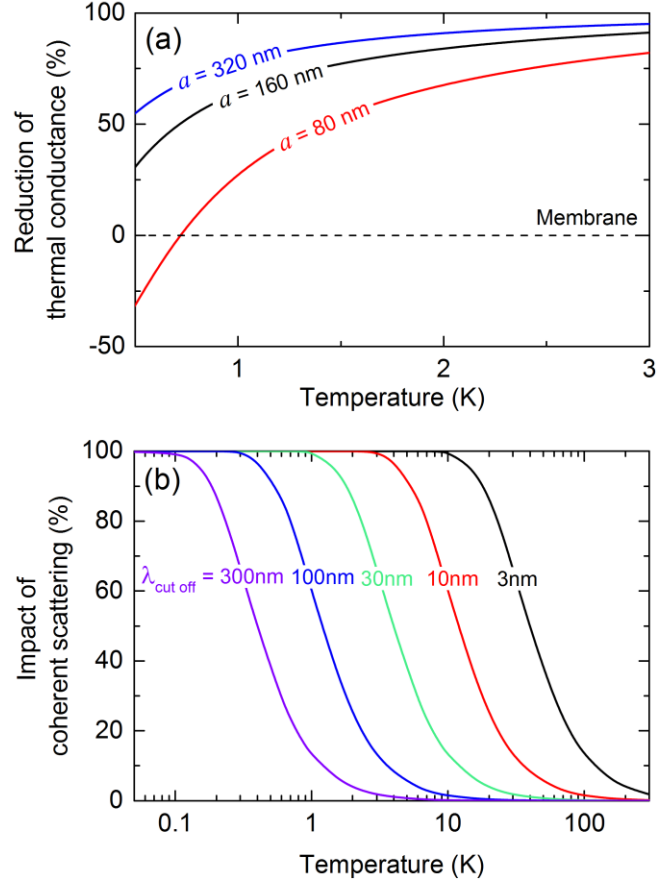


FIG. 6. (Color online) (a) Reduction in thermal conductance $(G_{\text{Mem}} - G_{\text{PnC}}) / G_{\text{Mem}}$ in square lattice phononic structures ($h = 80 \text{ nm}$, $r/a = 0.4$) with different periods ($a = 80, 160, \text{ and } 320 \text{ nm}$), as compared to an unpatterned membrane, as a function of temperature. (b) Impacted portion of thermal conductance (G_{coherent}) in square lattice phononic crystals ($h = 80 \text{ nm}$, $r/a = 0.4$, $a = 160 \text{ nm}$) as a function of temperature for different values of the cutoff wavelength.

On the other hand, the wave picture of phonons, discussed in this work, is relevant probably only at relatively low temperatures, when the thermal phonon wavelengths are comparable to the characteristic size of the structure [11,12,24]. Indeed, at room temperature, the phonon wavelength is in the 1–5 nm range [32], which is comparable to the surface roughness, so the phonon boundary scattering is mostly incoherent (or diffusive) [24]; at low temperatures, thermal phonon wavelengths become longer, and coherent phonon scattering may not only play an important role, but even fully control the phonon transport [11].

To discuss the role of coherent scattering at different temperatures, we assume the existence of a cutoff wavelength (λ_{cutoff}) below which phonon scattering is purely incoherent [12]. Such a cutoff wavelength is assumed typically to be at least bigger than the surface roughness. Moreover, according to the formula of Ziman [33]: $p = \exp(-16\pi^3\delta^2/\lambda^2)$, the wavelength (λ) should be at least of the order of 100 nm to achieve a specularity (p) of 0.5, for a surface roughness (δ) of a few nanometers. In phononic nanostructures, the cutoff wavelength is often approximated by the characteristic size of the structure, which is the period [24] or neck size [12,34] of the phononic crystal. To estimate the part of heat affected by coherent scattering, we calculate the ratio of the part of the heat flux spectrum up to λ_{cutoff} to the entire spectrum (Eq. 3). Here, to obtain the heat flux at high temperatures, we approximate the group velocity and DOS by linear fits and extend them to high frequencies.

$$G_{coherent}(T) = \frac{\int_0^{\lambda_{cutoff}} Q(\lambda, T) d\lambda}{\int_0^{\infty} Q(\lambda, T) d\lambda} \quad (3)$$

Figure 6(b) shows the impacted portion of thermal conductance ($G_{coherent}$) as a function of temperature for different values of the cutoff wavelength (λ_{cutoff}). These data demonstrate that, in structures with $\lambda_{cutoff} > 100$ nm, coherent scattering significantly impacts the thermal conductance only at temperatures of about 1 K. This finding is in agreement with the experimental observations reported by Zen *et al.* [11] where the thermal conductance starts to deviate from a completely coherent picture above 0.4 K. At room temperature, a noticeable impact can be produced only by structures with λ_{cutoff} shorter than a few nanometers, which implies unrealistic conditions of very small characteristic sizes and/or the absence of surface roughness. These estimations of the impact of coherent scattering are in agreement with similar considerations involving the random path tracing method [34]. Therefore, at room temperature, coherent scattering probably plays a much less important role than other scattering mechanisms. Thus, the applications of coherent phonon control in phononic crystals are probably limited to low-temperature devices such as transition edge sensors [35].

V. CONCLUSION

We have investigated the impact of structure design on the efficiency of coherent phonon scattering in 2D phononic crystals. Our results demonstrate that thermal conductance of phononic crystals shows a decrease as a function of the period (a) and radius-to-period (r/a) ratio. This implies that, contrary to the case of incoherent surface scattering, the period of the structure should be increased to ensure the lowest thermal conductance. Thus, to study coherent scattering experimentally, we should compare structures with different periods, but with the same surface-to-volume ratio. Moreover, thermal conductance reduction does not depend on the lattice type, despite differences in symmetry and geometry. Therefore, the lattice choice can be made to ensure strong incoherent scattering (hexagonal lattice) or rigidity of the structure (honeycomb lattice). Our study also demonstrates that, although the reduction of thermal conductance is increased with temperature, coherent scattering plays an important role in realistic nanostructures only at relatively low temperatures.

ACKNOWLEDGMENTS

This work was supported by the Project for Developing Innovation Systems of the Ministry of Education, Culture, Sports, Science and Technology (MEXT), Japan and by KAKENHI (25709090 and 15K13270).

REFERENCES

- [1] G. Schierning, Phys. Status Solidi **211**, 1235 (2014).
- [2] M. Maldovan, Nature **503**, 209 (2013).
- [3] J. Gomis-Bresco, D. Navarro-Urrios, M. Oudich, S. El-Jallal, A. Griol, D. Puerto, E. Chavez, Y. Pennec, B. Djafari-Rouhani, F. Alzina, A. Martínez, and C. M. S. Torres, Nat. Commun. **5**, 4452 (2014).
- [4] J. O. Vasseur, P. A. Deymier, B. Djafari-Rouhani, Y. Pennec, and A.-C. Hladky-Hennion, Phys. Rev. B **77**, 085415 (2008).
- [5] Y. Pennec, J. O. Vasseur, B. Djafari-Rouhani, L. Dobrzański, and P. A. Deymier, Surf. Sci. Rep. **65**, 229 (2010).
- [6] R. Pourabolghasem, A. Khelif, S. Mohammadi, A. A. Eftekhar, and A. Adibi, J. Appl. Phys. **116**, 013514 (2014).
- [7] D. Feng, D. Xu, G. Wu, B. Xiong, and Y. Wang, Appl. Phys. Lett. **103**, 151906 (2013).
- [8] Y. Pennec, B. Djafari Rouhani, E. H. El Boudouti, C. Li, Y. El Hassouani, J. O. Vasseur, N. Papanikolaou, S. Benchabane, V. Laude, and A. Martinez, Opt. Express **18**, 14301 (2010).

- [9] S. Sadat-Saleh, S. Benchabane, F. I. Baida, M.-P. Bernal, and V. Laude, *J. Appl. Phys.* **106**, 074912 (2009).
- [10] S. Mohammadi, A. A. Eftekhar, A. Khelif, W. D. Hunt, and A. Adibi, *Appl. Phys. Lett.* **92**, 221905 (2008).
- [11] N. Zen, T. A. Puurinen, T. J. Isotalo, S. Chaudhuri, and I. J. Maasilta, *Nat. Commun.* **5**, 3435 (2014).
- [12] E. Dechaumphai and R. Chen, *J. Appl. Phys.* **111**, 073508 (2012).
- [13] R. Anufriev and M. Nomura, *Phys. Rev. B* **91**, 245417 (2015).
- [14] P. E. Hopkins, C. M. Reinke, M. F. Su, R. H. Olsson, E. a Shaner, Z. C. Leseman, J. R. Serrano, L. M. Phinney, and I. El-Kady, *Nano Lett.* **11**, 107 (2011).
- [15] B. L. Davis and M. I. Hussein, *Phys. Rev. Lett.* **112**, 055505 (2014).
- [16] M. Nomura, J. Nakagawa, Y. Kage, J. Maire, D. Moser, O. Paul, M. Nomura, J. Nakagawa, Y. Kage, J. Maire, and D. Moser, *Appl. Phys. Lett.* **106**, 143102 (2015).
- [17] W. Fon, K. C. Schwab, J. M. Worlock, and M. L. Roukes, *Phys. Rev. B* **66**, 045302 (2002).
- [18] M. Nomura, Y. Kage, J. Nakagawa, T. Hori, J. Maire, J. Shiomi, R. Anufriev, D. Moser, and O. Paul, *Phys. Rev. B* **91**, 205422 (2015).
- [19] A. I. Hochbaum, R. Chen, R. D. Delgado, W. Liang, E. C. Garnett, M. Najarian, A. Majumdar, and P. Yang, *Nature* **451**, 163 (2008).
- [20] Y.-J. Han, *Phys. Rev. B* **54**, 8977 (1996).
- [21] J.-K. Yu, S. Mitrovic, D. Tham, J. Varghese, and J. R. Heath, *Nat. Nanotechnol.* **5**, 718 (2010).
- [22] J. Tang, H.-T. Wang, D. H. Lee, M. Fardy, Z. Huo, T. P. Russell, and P. Yang, *Nano Lett.* **10**, 4279 (2010).
- [23] V. Lacatena, M. Haras, J.-F. Robillard, S. Monfray, T. Skotnicki, and E. Dubois, *Appl. Phys. Lett.* **106**, 114104 (2015).
- [24] A. Jain, Y.-J. Yu, and A. J. H. McGaughey, *Phys. Rev. B* **87**, 195301 (2013).
- [25] K. Busch and S. John, *Phys. Rev. E* **58**, 3896 (1998).
- [26] A. Majumdar, *J. Heat Transfer* **115**, 7 (1993).
- [27] T. Kühn, D. V. Anghel, J. P. Pekola, M. Manninen, and Y. M. Galperin, *Phys. Rev. B* **70**, 125425 (2004).
- [28] S. Mohammadi, A. A. Eftekhar, A. Khelif, H. Moubchir, R. Westafer, W. D. Hunt, and A. Adibi, *Electron. Lett.* **43**, 898 (2007).
- [29] M. Maldovan and E. L. Thomas, *Appl. Phys. Lett.* **88**, 251907 (2006).
- [30] M. Nomura and J. Maire, *J. Electron. Mater.* **44**, 1426 (2014).
- [31] J. Maire and M. Nomura, *Jpn. J. Appl. Phys.* **53**, 06JE09 (2014).
- [32] K. Esfarjani, G. Chen, and H. T. Stokes, *Phys. Rev. B* **84**, 085204 (2011).

- [33] J. M. Ziman, *Electrons and Phonons: The Theory of Transport Phenomena in Solids* (Clarendon, Oxford, 1962).
- [34] A. M. Marconnet, T. Kodama, M. Asheghi, and K. E. Goodson, *Nanoscale Microscale Thermophys. Eng.* **16**, 199 (2012).
- [35] I. J. Maasilta and T. Kühn, *J. Low Temp. Phys.* **151**, 64 (2008).